


The Design and Building of a Hexapod Robot with Biomimetic Legs

Min-Chan Hwang *, Feifei Liu, Jie Yang  and Yuanzhang Lin

School of Electrical Engineering and Automation, Jiangxi University of Science and Technology, Ganzhou 341000, China

* Correspondence: aemchwang@163.com; Tel.: +86-1777-075-4280

Received: 1 June 2019; Accepted: 9 July 2019; Published: 11 July 2019



Abstract: A hexapod robot with biomimetic legs was built to implement a distributed control system, where a mechanism is proposed to serve as the central pattern generator and a computer to act as the brain-stem, cooperating with the central pattern generator through wireless communication. The proposed mechanism is composed of two modules, i.e., the tripod gait generator and the Theo Jansen Linkage. The tripod gait generator is a device that uses a single motor to generate a tripod gait, while the Theo Jansen Linkage rhythmically executes the legged motion. In a sense, we are trying to implement the locomotion of a robot by means of a hybrid computational system, including the mechanism part and the electronic processors part. The complex mathematical function of the foot movement is realized by the ensemble of links of the Theo Jansen Linkage, so as to alleviate the computational burden. Besides, the proposed design, based on non-collocated actuators, is intended to minimize the number of actuators while reducing the building cost of the robot.

Keywords: central pattern generator; Theo Jansen Linkage; non-collocated actuators

1. Introduction

The grounds of construction sites or factories are often muddy or scattered with debris. Under such circumstances, wheeled vehicles used for material handling might be easily blocked by obstacles or experience skidding on the muddy grounds. Hence, this inspires us to pursue the development of a hexapod robot to replace a wheeled vehicle. However, robots are complex and expensive machines, consisting of many actuators, sensors, transmissions, and hardware. Therefore, a method of developing a hexapod robot to reduce the cost by means of using a minimal number of actuators is proposed. In this article, a hexapod robot was conceived, designed, and built.

In the development of a legged robot, there are two primary concerns, i.e., how to generate a stable gait, so that the robot can walk without tumbling, and how to perpetually generate stable gaits. Regarding the first concern, McGhee and Frank [1,2] proposed the COG (center of gravity projection) method in 1968, stating that the legged robot is statically stable if the horizontal projection of its COG lies within the support polygon, which is defined as the convex polygon formed by connecting the footprints. Orin [3] generalized the COG method in 1976, proposing the COP (center of pressure) method, where a robot is dynamically stable if the projection of the COG, along the direction of the resultant force acting on the COG, lies within the support polygon. In 1969, Vukobratovic and Juricic [4,5] further proposed a method in favor of the biped robot called the ZMP (zero moment point) method, where a robot is stable if the moment about the COP, at its supporting foot, is zero. As to the second concern, many rhythmic movements such as locomotion, respiration, swallowing, etc., in animals, have been found to be produced by a CPG (central pattern generator) [6–11].

Neuroscientists [12] have employed a variety of techniques, including anatomical, behavioral, physiological methods, etc., to investigate the specific neural circuits and discover the mapping function

in those circuits. One notable study on the locomotion of the salamander [13] proposed the CPG model based on nonlinear oscillators instead of neural network oscillators, presented numerical as well as mechanical simulations, and successfully constructed a salamander-like robot. Some studies [14–16] have addressed to the locomotion of hexapods with CPG and established mathematical models not only including the rhythmic generator, but also the interlimb coordinator, so that the hexapod can adapt to variant terrains by gait transition. Beyond bio-inspiration, a new trend of research that is noteworthy is the merging of natural and artificial components, which is defined as bio-hybrid organisms [17,18], also called bio-robots, in which an artificial component or a biological organ is incorporated into an animal or robot, respectively. These studies even investigate how the artificial agent interacts with an animal individual or a population. So far, all studies have relied on electronic circuits or processors to implement the locomotion of legged robots.

Computers have always been thought of as nothing more than electronic devices, which is not necessarily the case. Recalling the evolution of computer science, the earlier computing devices, called calculators, invented by Blaise Pascal of France (1642) and G.W. Leibniz of Germany (1671), were built with the technology of gears. In fact, they were mechanical calculators, where data was represented through gear positioning and entered mechanically, by adjusting the initial gear positions. The output of the calculators was achieved by observing the final gear positions. Therefore, mechanical devices can be regarded as computational processors, as long as they execute certain mathematical operations. This was the inspiration to create a mechanism, or mechanical computational processor, to complement the electronic processors.

Moreover, neuroscience discovered that the CPG, located in the spinal cord, is an autonomous device, almost requiring neither the peripheral sensor feedback, nor the regulation command from the brain-stem. Therefore, a hexapod robot with biomimetic legs was built, to implement such a distributed control system, where a mechanism is proposed to serve as the CPG and a computer acts as the brain-stem, to command the autonomous device through wireless communication. In a sense, we are trying to implement the locomotion of a robot by means of a hybrid computational system, including a mechanism and electronic computers. The proposed mechanism comprises two modules, i.e., the tripod gait generator and the Theo Jansen Linkage. The tripod gait generator is a device that uses a single motor to generate a tripod gait that couples the middle leg on one side with the front and rear leg on the other side, while the TJL (Theo Jansen Linkage) rhythmically executes the legged motion.

The TJL was first introduced by Theo Jansen in 1990, where he presented a strandbeest [19], elegantly achieving a bio-inspired locomotion. This soon drew the attention of robotics researchers [20–25]. The TJL adopted in this paper is an eight-bar linkage. The interesting point is that the foot movement is a complex mathematical function, from a crank to a rocker. Nonetheless, it can be simply realized by the combination of these eight links. Consider that, if the same function is processed by an electronic device, it will consume a great amount of computational time and memory resources. Therefore, our proposed mechanism can alleviate the computational burden. Moreover, most hexapods are designed with collocated actuators, i.e., each joint is mounted with an actuator, so the number of actuators is usually high, reaching even 18, in number. Using a high number of actuators leads to many adverse effects, including increased challenge for the algorithms to control legged motions, degradation of the loading capacity, and increase of the construction cost. Hence, the present proposed design is based on non-collocated actuators, so as to minimize the number of actuators while reducing the building cost of the robot.

2. Mechanical Structure

The TJL can be built using either 8 or 12 links, depending on the fabrication method of two triangular links of the TJL. If each triangular link is machined into a whole piece, the TLJ is an 8-bar linkage, whereas if each of them is assembled by three straight bars, the TLJ is a 12-bar linkage. The TJL, as adopted in this paper, is the eight-bar linkage option. It can be considered as a device to implement

the mathematical function for the legged motion, as will be presented in the Kinematics section. As illustrated in Figure 1, the complexity of the foot movement implementation is not in any way reduced, but rather a passing from the computer to the mechanism occurs, i.e., coding is replaced by component designing. Once the ensemble of links is determined, it can generate a deterministic orbit.

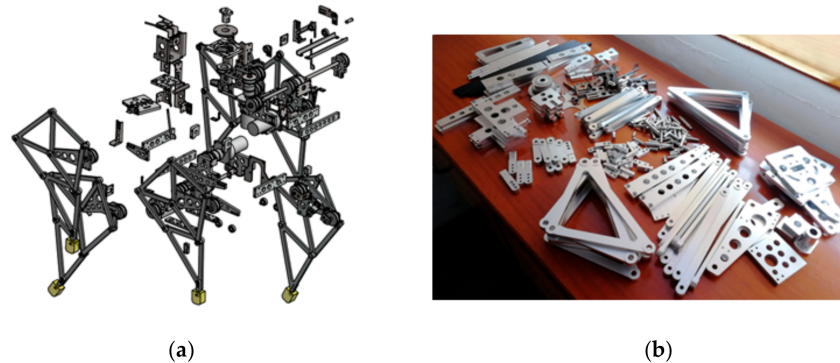


Figure 1. (a) Assembly drawing. (b) Mechanical components.

The hexapod robot (Figure 2a) is divided into three modules, i.e., an upper deck, a bottom deck, and a swivel connecting the both of them (Figure 2b). In regard to manufacturing or maintenance, we should avoid diversifying the components design-wise. Instead, it is more practical to design the components shared by different modules. Hence, both decks are designed according to the same structure except their legs, which are mounted with opposing orientation. Therefore, it is adequate to study just one of them, while the bottom deck will be used for illustration purposes.

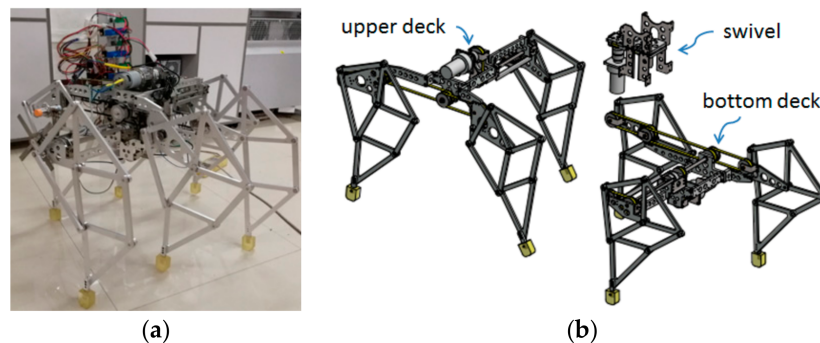


Figure 2. (a) Completed hexapod robot. (b) Three major modules.

The bottom deck consists of one tripod gait generator and three TJLs. The tripod gait generator is a module dispatching power from a motor to three legs (Figure 3a), each of which is a TJL.

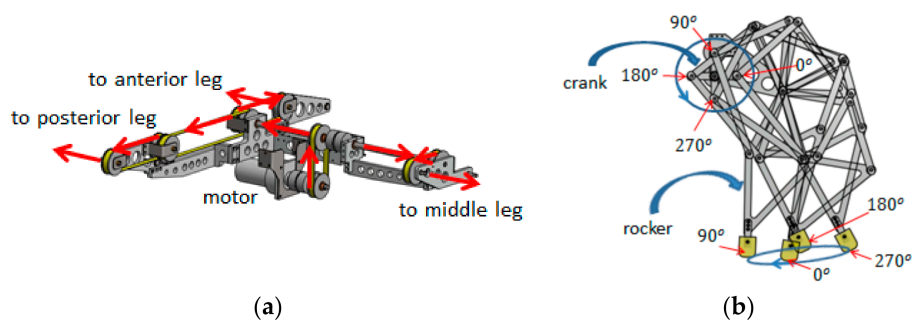


Figure 3. (a) The module of a tripod gait generator. (b) Theo Jansen leg with four phases.

Let the crank of a TJL pose at four different angles, i.e. 0° , 90° , 180° and 270° . Consequently, these four postures of the TJL are superimposed, showing the motion of the rocker in relation to the crank. In Figure 3b, the tip of the rocker draws an orbit, in a sense opposite to the rotation of the crank, as the four phase angles of the crank, labeled at the foot trajectory, help acknowledge how the rocker is related to the crank during motion.

The tripod gait module is also a device which couples the middle leg on one side with the front and rear on the other side, to rhythmically generate tripod gaits. The locomotion of the hexapod is achieved by alternating two support polygons, each being the triangle connecting the tips of the rockers (Figure 4).

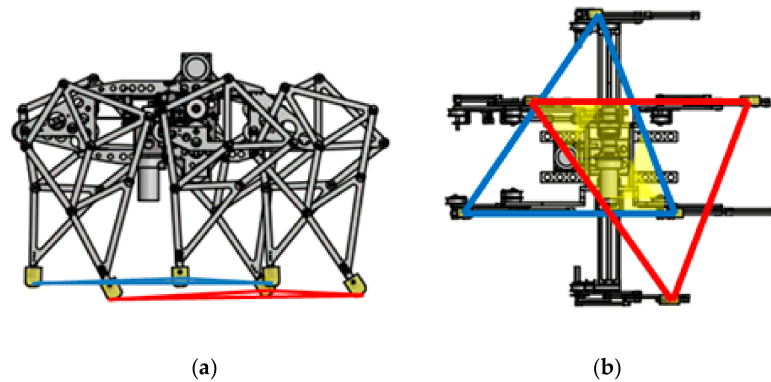


Figure 4. (a) Lateral view of two support triangles. (b) Bottom view of two support triangles.

3. Kinematics

The kinematics of the TJL (Figure 5) can be derived according to the Denavit–Hartenberg [26] convention, along with certain trigonometric constraints. Hence, the orbit of the foot tip is a function of the input variable θ , also referred to as the crank angle, and defined as follows:

$$x(\theta) = A_1 \cos \theta_1 + L_4 \cos(\theta_1 + \theta_2) + S_2 \cos(\theta_1 + \theta_2 + \theta_3) \quad (1)$$

$$y(\theta) = -[A_1 \sin \theta_1 + L_4 \sin(\theta_1 + \theta_2) + S_2 \sin(\theta_1 + \theta_2 + \theta_3)] \quad (2)$$

where

$$S_0 = \sqrt{S_x^2 + S_y^2} \quad (3)$$

$$\beta_1 = \tan^{-1} \left(\frac{S_y}{S_x} \right) \quad (4)$$

$$\beta_2 = \beta_1 + \theta \quad (5)$$

$$S_1 = \sqrt{S_0^2 + L_1^2 - 2L_1 S_0 \cos \beta_2} \quad (6)$$

$$\beta_3 = \tan^{-1} \left(\frac{L_1 \sin \beta_2}{S_0 - L_1 \cos \beta_2} \right) \quad (7)$$

$$\beta_4 = \cos^{-1} \left(\frac{S_1^2 + A_2^2 - L_2^2}{2S_1 A_2} \right) \quad (8)$$

$$\beta_5 = \cos^{-1} \left(\frac{A_1^2 + A_2^2 - A_3^2}{2A_1 A_2} \right) \quad (9)$$

$$\theta_1 = \beta_1 + \beta_3 + \beta_4 + \beta_5 - 180^\circ \quad (10)$$

$$\beta_6 = \cos^{-1} \left(\frac{S_1^2 + L_4^2 - L_3^2}{2S_1 L_4} \right) \quad (11)$$

$$\theta_2 = \beta_7 = 360^\circ - (\beta_4 + \beta_5 + \beta_6) \quad (12)$$

$$\beta_9 = \cos^{-1} \left(\frac{B_1^2 + B_3^2 - B_2^2}{2B_1B_3} \right) \quad (13)$$

$$\beta_{10} = \tan^{-1} \left(\frac{(B_3 + E) \sin \beta_9}{B_1 - (B_3 + E) \cos \beta_9} \right) \quad (14)$$

$$\theta_3 = 180^\circ - (\beta_7 + \beta_{10}) \quad (15)$$

$$S_2 = \sqrt{(B_3 + E)^2 + B_1^2 - 2B_1(B_3 + E) \cos \beta_9} \quad (16)$$

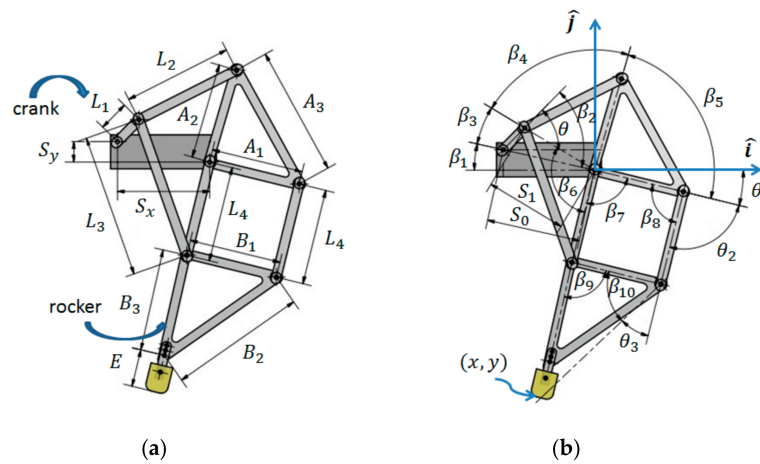


Figure 5. Theo Jansen Linkage (a) dimensions and (b) geometrical variables.

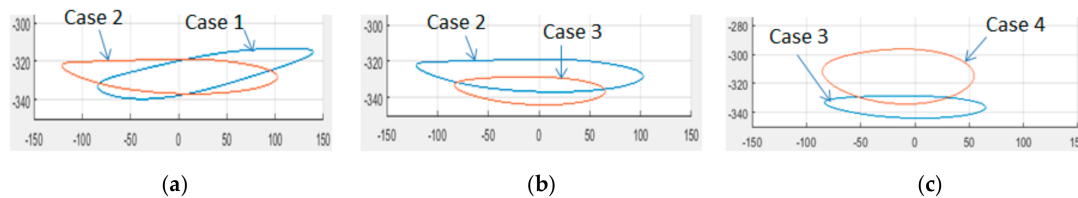
The orbits patterns produced by TJLs might end up as bell curves, ovals, sharp-pointed ovals, or lemniscates, depending on the assembly of their variant sizes. Not all generated orbits are suitable to serve as foot trajectories for the legged robots. Hence, dimensioning the TJL appropriately is nontrivial, since the orbits patterns generated by a TJL may vary according to its assembled dimensions, and can be cast into four groups, including bell curves, ovals, sharp-pointed ovals, and lemniscates. In general, the ovals or bell orbits are legitimate, while the sharp-pointed ovals are partly legitimate, and the lemniscates are illegitimate. After analyzing and balancing requirements, the design data of L_4 , A_1 , A_2 , A_3 , B_1 , B_2 , B_3 , E , S_x , and S_y were set to be 140, 135, 140, 190, 135, 200, 150, 55, 135, and 30, respectively.

In Table 1, four cases of links with different lengths: L_1 , L_2 , and L_3 , are illustrated along with the respective data of foot trajectories, demonstrating how they are influenced by the variant links. Although all four cases include legitimate orbits, there are some other concerns to be taken into account in order to achieve a satisfactory design. The maximum step size is defined as the distance between the leftmost point and the rightmost point. Similarly, the maximum step height is defined as the distance between the topmost point and the bottommost point. Although both of these are different from the actual step size and height, they are able to show the effectiveness of the following actions. Regarding the actual step size and height, a slightly more complicated calculation is required, which will be presented in the next section.

Indicatively, in the trajectory of Case 1 (Figure 6a), where the inclination is too deep, the corrective measure, taken by Case 2, is to reduce the lengths of L_2 and L_3 . Nonetheless, as mentioned earlier, the stability of the hexapod is ensured by the intersection of two support polygons. Given the fact that, the larger the stride, the smaller the intersected polygon will be, the hexapod will eventually be destabilized if the stride is too large. In order to ensure stability, the action taken by Case 3 is to shorten the step size, by reducing the length of L_1 (Figure 6b). After these efforts, the hexapod is ready to walk. However, its step height is relatively small, so the further action, taken by Case 4, is to increase the step height (Figure 6c), by the fourth set of data in Table 1.

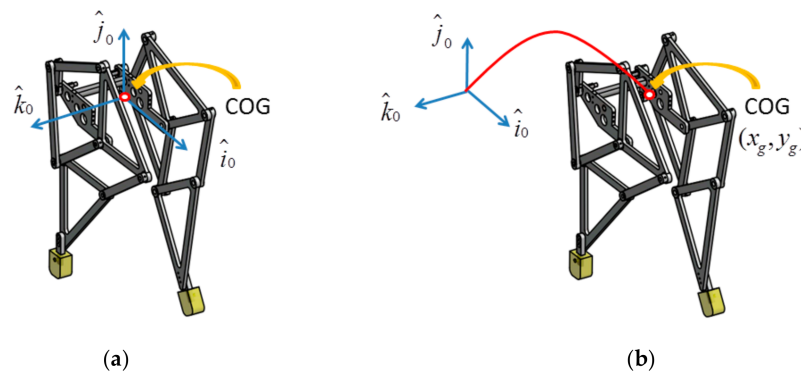
Table 1. Four sets of design data for L_1 , L_2 , and L_3 .

Case	L_1 (mm)	L_2 (mm)	L_3 (mm)	Max. Step Size (mm)	Max. Step Height (mm)
1	45	160	210	223.6	26.2
2	45	172	200	223.8	18.1
3	30	172	200	148.8	15.4
4	30	150	164	139.8	37.8

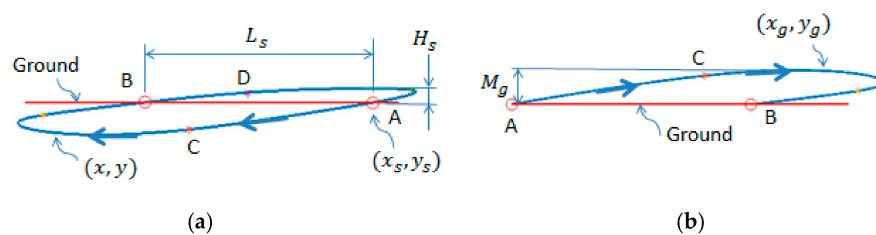
**Figure 6.** Actions: (a) inclination decreased, (b) step size reduced, and (c) step height increased.

4. Locomotion

The locomotion of this hexapod can be analyzed in terms a simplified model (Figure 7), a biped robot with absolute stability, by regarding the left and right legs of the biped version as the legs of the upper and lower deck of the hexapod, respectively. Following this, the locomotion of the robot can be characterized by the motion of its COG (Center of Gravity).

**Figure 7.** A simplified model of the robot: (a) Initial configuration and (b) motion of the center of gravity Projection (COG).

The cranks of the left and right legs will keep apart by 180° during rotation, and Figure 8 illustrates how the motion of the COG relates to the foot trajectory where (x, y) , (x_g, y_g) , L_s , H_s , and M_g stand for the foot trajectory, the motion of the COG, the step size, the step height, and the fluctuated amplitude, respectively.

**Figure 8.** (a) Foot trajectory. (b) Motion of COG.

The robot is initially at rest with one foot standing at point A, while another foot stands at point B. The coordinates of point A are denoted as (x_s, y_s) , which is associated with the crank angle θ_s ,

while the crank angle of point B is 180° apart from θ_s , i.e., $\theta_s + \pi$. Hence, point A can be obtained by determining the crank angle θ_s , where the height of point A is equal to the height of point B, using Equations (1)–(16). Following, the step size L_s , step height H_s , and fluctuated amplitude M_g , are calculated and listed in Table 2.

Table 2. Characteristics of foot trajectories related to four sets of design data.

Case	θ_s ($^\circ$)	L_s (mm)	H_s (mm)	M_g (mm)	H_s/M_g
1	317.4	131.3	8.0	18.2	0.44
2	234.3	201.4	3.8	14.3	0.27
3	241.8	141.8	4.6	10.8	0.43
4	246.9	135.4	12.3	25.5	0.48

As the foot engages on point A, it pushes the robot forward, as well as upward. Hence, by mirroring the part of foot trajectory ABC, with respect to the horizontal and vertical axes, the locus of the COG is derived, yielding the following equations:

$$x_g(\theta) = nL_s + x_s - x(\theta - n\pi) \quad (17)$$

$$y_g(\theta) = y_s - y(\theta - n\pi) \quad (18)$$

$$n = \left\lfloor \frac{\theta - \theta_s}{\pi} \right\rfloor \quad (19)$$

where, the bracket $\lfloor \cdot \rfloor$ yields the maximum integer, no greater than the value it contains.

The locomotion of the robot, i.e., rhythmically alternating one foot with another, can be well characterized by the locus of its COG, using Equations (17)–(19). The loci of the COG pertaining to four different cases are as shown in Figures 9–12.

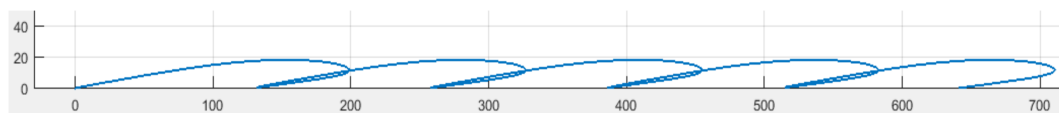


Figure 9. Locus of center of gravity for Case 1.

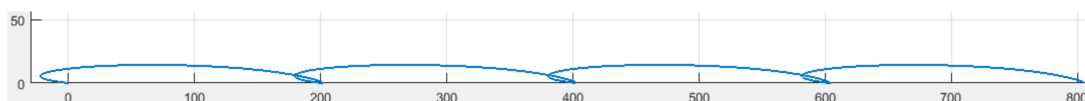


Figure 10. Locus of center of gravity for Case 2.

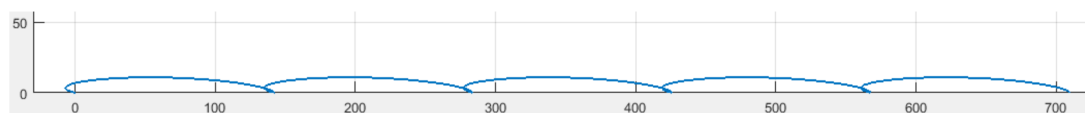


Figure 11. Locus of center of gravity for Case 3.

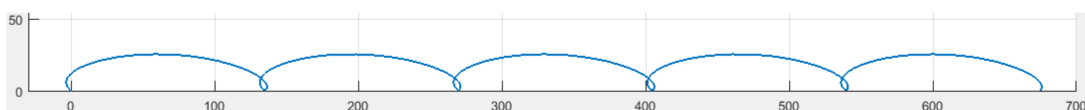


Figure 12. Locus of center of gravity for Case 4.

In Figure 9, the locus manifests that the robot will wobble significantly, while moving. This adverse effect arises from the fact that the foot trajectory, generated by the TJL in Case 1, exhibits large obliqueness. In an effort to improve this situation, the inclination of the orbit was reduced, causing a side effect

on the actual step size, i.e., an increase by 1.5 times (Figures 9 and 10). The maximum step sizes in Cases 1 and 2 (Table 1) are almost the same and the respective orbits (Figure 6a) are similar. Evidently, the actual step size is not only determined by the orbit itself, but also by the points where the feet meet the ground, i.e., point A and point B (Figure 8).

Moreover, the robot can change its azimuth by a swivel mechanism, located between the upper and bottom deck. In order to avoid mechanical collision, the swivel motor is limited to rotate within $\pm 15^\circ$. However, the robot is still able to manage turns greater than $\pm 15^\circ$ through a sequence of detailed maneuvers of its swivel and legs. An example is illustrated in Figure 13. Considering that the body and output shaft of the swivel motor are connected to the bottom and upper deck, respectively, the swivel motor has to reverse its output shaft, depending on which set of legs is standing on the ground, as the robot changes its azimuth. In Figure 13b, the swivel motor turns clockwise, to swing the upper deck in the same direction, while the legs of the bottom deck stand statically on the ground. In Figure 13c, the swivel motor turns counterclockwise to swing the bottom deck in the opposite direction, i.e., clockwise, when the legs of the upper deck stand statically on the ground.

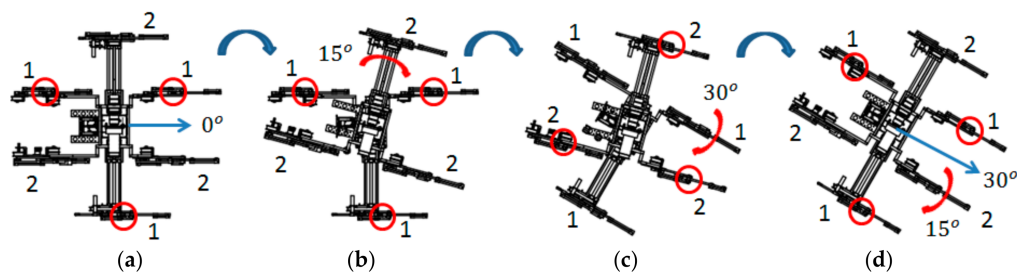


Figure 13. The robot changes its azimuth through a series of motions where the legs of the bottom deck and the upper deck are labeled as 1 and 2, respectively, while the red circles stand for the legs standing statically on the ground. (a) Initial posture. (b) The upper deck suspends its legs and makes a swing 15° clockwise, while the legs of the bottom deck stay on the ground. (c) The bottom deck suspends its legs and makes a swing 30° clockwise, while the legs of the upper deck stay on the ground. (d) The upper deck suspends its legs and makes a swing 15° clockwise, while the legs of the bottom deck stand on the ground.

5. Mechatronics of the Control System

Following the analysis and construction of the mechanism, the mechatronics of the control system (Figure 14), consisting of a microcontroller, drivers, sensors, and motors with gear trains, was built.

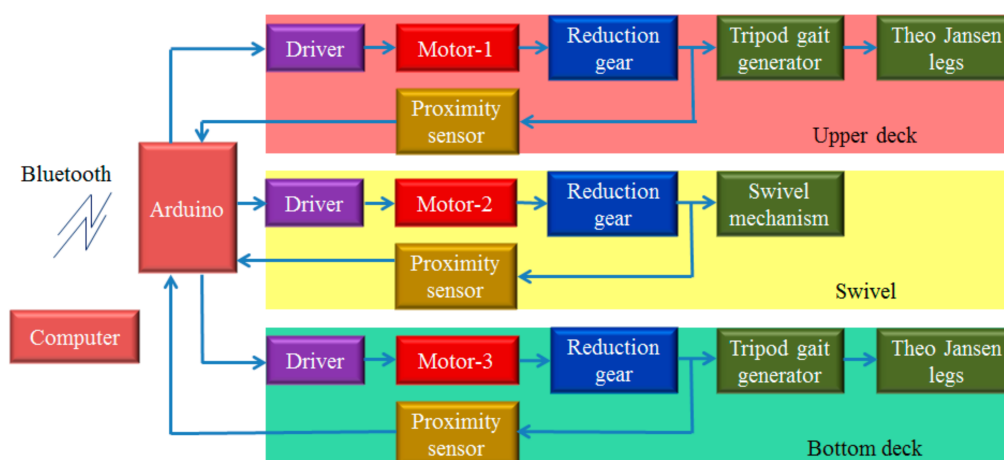


Figure 14. Block diagram of mechatronic system.

This part mainly controls the orientation of the swivel and the motions of the TJLs, with a phase of 180° between the two sets of cranks. The Arduino was chosen as the microcontroller for this project. Since the first Arduino [27] was introduced in 2005, it has become one of the most popular microcontrollers used by engineers and even large corporations. The appealing features of Arduino are mostly its openness and ease-of-use. It is worth mentioning that the programming of an embedded system is done according to cross-development principles, so that the code can run on a target board, different from the one where the code was built. The Arduino provides an integrated development environment (IDE) for users to edit, debug, and compile their application programs on a personal computer and then upload them to the Arduino board for execution.

In Figure 15, the crank of the TJL is attached through four metal blades, evenly partitioning the circumference into four quarters. The proximity sensor, CHII B LJ18A3-10-Z/BY, is used to detect four phases of the crank, based on which the Arduino is able to keep the two sets of cranks apart, at 180° , during operation. Regarding the control of the swivel (Figure 16), specific care needs to be taken to avoid mechanical collision. First, one system, consisting of a proximity sensor, CHII B LJ12A3-4-Z/BY, and three metal blades, is installed to receive feedback on the azimuth of the swivel. Second, another system, using two limited switches as a safety guard to assure that the range of operation is maintained, is installed. When the swivel reaches its maximum range, it will push the leverage of the limited switch, so as to cut off the power of the swivel motor immediately. Without the safety guard system, the catastrophe of a mechanical collision is inevitable in developing the application programs. Regarding the DC motors, there are two motors with specifications of 12 V, 2 A, 35 W, 30 rpm, and 25.47 kg-cm, used for the TJLs and one motor with specifications of 12 V, 2 A, 35 W, 10 rpm, and 76.4 kg-cm, used for the swivel. The drivers are all in typical H-bridge with specifications of 12–36 V, 10 A, and 120 W.

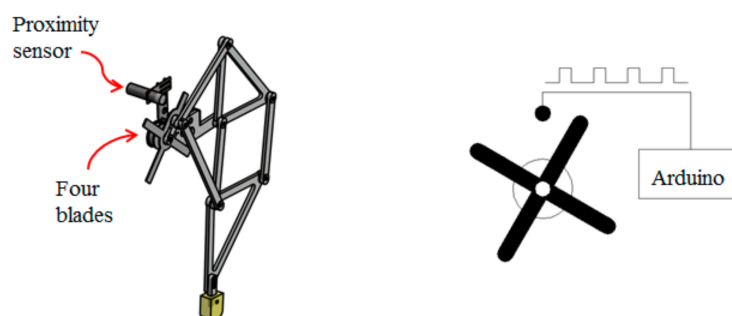


Figure 15. Sensor system to detect the phases of the crank.

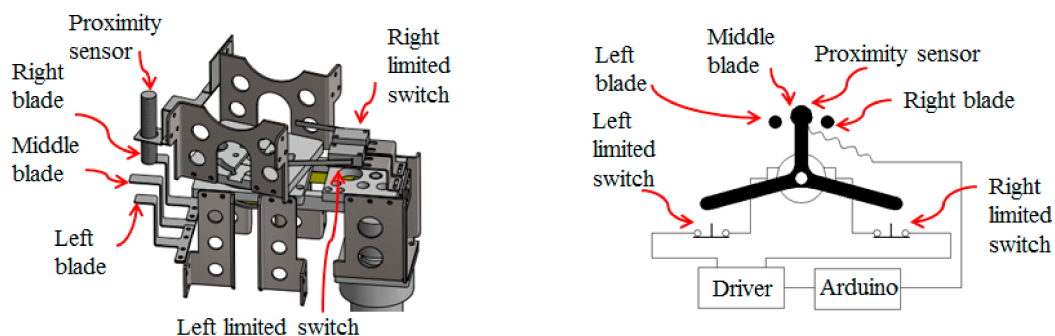


Figure 16. Sensor system to detect the azimuth of the swivel and the safety guard system.

In this project, Bluetooth (BT) was used to establish wireless communication between the computer and the Arduino. Bluetooth is a wireless technology standard, IEEE 802.15.1, for exchanging data between fixed and mobile devices over short distances, most often within 10 m, using short-wavelength

UHF (Ultra High Frequency) radio waves, in the industrial, scientific and medical radio bands, from 2.400 to 2.485 GHz, and in personal networks.

AT (Attention), commands are instructions used to control a modem. Every command line starts with “AT” or “at,” which is why modem commands are called AT commands. Some AT commands used to configure the BTs and a portion of Arduino program, related to the wireless communication, are provided in Table 3. The BTs need to be set up before communication. First, the KEY-pin is set to high, before powering up the BT. As the power is turned on, the BT enters a setting mode, where its LED blinks with a period of four seconds, i.e., light on for two seconds and light off for two seconds. Then, AT commands are used to configure the baud rate, parity, stop bit, password, master/slave, binding address, etc. Following this, the power is turned off and the KEY-pin is set to low. As the power is turned on again, the BTs enter a standby mode, where they blink every second, in an attempt to pair up. At successful pairing up, both BTs get into the communication mode, where they blink twice for two seconds and light off for two seconds. Upon completion of the mechatronic control system, programs were developed, where the Arduino side mainly awaits the commands from the computer and keeps two sets of cranks apart at 180° during operation, while the computer side sends wireless commands to the Arduino. Since the legged motion has been realized by the mechanism, there is no need to develop a sophisticated algorithm in Arduino.

Table 3. AT Commands and Arduino program related to communication.

AT Commands	Arduino Program Paradigm
AT+ADDR?	header: #include <SoftwareSerial.h>
AT+PSWD?	setup: SoftwareSerial BTSerial(8, 7); //RX, TX
AT+ROLE?	Serial.begin(38400);
AT+CMODE=0/1	BTSerial.begin(38400);
AT+UART=38400,0,0	Loop: if(BTSerial.available()){
AT+BIND=98D3,31,206801	ch=BTSerial.read();
AT+BIND?	...
...	Serial.write(ch);}

In Figure 17, a sequence of snapshots of the hexapod robot, as tested on site, is illustrated. The appealing feature of this robot is that it is reliable and robust. Even if it runs out of battery or an electronics failure occurs, it can still stand because the tripod gaits are generated by the mechanism, instead of the computer.

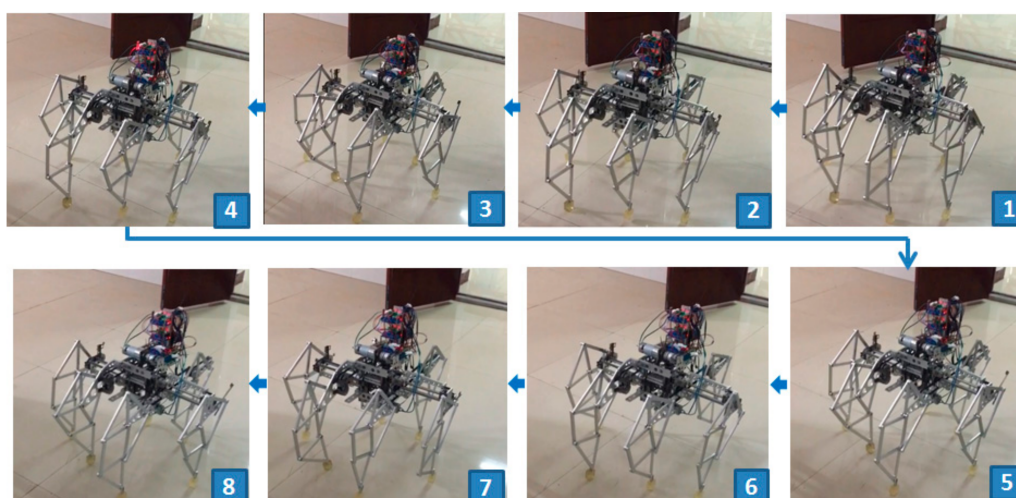


Figure 17. Snapshots of the hexapod robot in motion.

6. Comparison to Existing Hexapods

For the sake of comparison, an overview of existing hexapod robots is conducted in this section. Since the first hexapod robot with electric drivers and a computer-controller [28] was built in 1972, a variety of hexapod robots have been constructed according to varying technologies and design principles. Several hexapod robots limited to 14 kg at maximum are listed in Table 4.

Table 4. A variety of hexapod robots.

Year	Robot Name	Actuator No.	Power (W)	Mass (Kg)	Length (mm)	Width (mm)	Height (mm)	Remarks
2000	Biobot	18	NA ¹	11	580	140	230	Locomotion over rough terrain
2001	Hamlet	18	52	13	400	280	400	Force and position control
2001	Rhex	6	100	7	530	200	150	Reduced actuators
2002	Sprawlita	12	NA	0.27	160	NA	NA	Inspired on cockroaches
2004	Genghis	12	NA	1	400	150	NA	Developing of a reactive controller
2005	Bill-Ant-p	18	25	2.3	470	330	160	Bio-inspired robot
2006	Gregor I	16	25	1.2	300	90	40	Inspired on cockroaches
2006	RiSE	12	NA	3.2	410	NA	NA	Hexapod climbing robot
2017	Hexapod-I	3	7	4.5	712	641	189	Minimal number of actuators
2018	Hexapod-II	3	35	14	775	694	512	Minimal number of actuators

¹ NA: not available.

Biobot [29], inspired to the cockroach, was a hexapod with a great speed and agility. Hamlet [30] was built to study force and position control on uneven terrain. RHex [31], designed in mechanical simplicity and having only six actuators, can achieve fast and robust forward locomotion. Sprawlita [32] was based on functional principles derived from biomechanical studies of the cockroach to achieve a fast run. Genghis [33] presented an incremental method for building robot control systems analogous to evolution of the organism, i.e., each one being a strict augmentation of the previous one, which control a six legged walking machine. Bill-Ant-p [34], based on ants' behavior, was developed and consisted of 18 degrees of freedom for locomotion, i.e., each leg with three actuators and one force-sensing foot. Gregor I [35] is also a bio-inspired hexapod where the locomotion control is based on the CPG and the core of its control architecture is the Cellular-Nonlinear-Network CPG chip. RiSE [36] is a hexapod robot which is able to climb on a variety of vertical surfaces. It employs arrays of miniature spines to catch on surface asperities.

The hexapod robot of this article, named Hexapod-II, is an improved version of the Hexapod-I [37]. The difference between Hexapod-I and Hexapod-II lies in their biomimetic legs. The former uses four-bar linkages, while the latter uses the TJLs. The four-bar linkage can only generate a circular orbit, which leads the hexapod robot to move in a way with a larger fluctuation (Figure 18) because its step height is always one half of its step size, as two tripod gaits are alternated with a phase lag of 180°. In contrast, the TJL generates an ellipse-like trajectory which possesses a transversal axis longer than the lateral axis, so that it can achieve energy efficient walking, as compared to the circular orbit generated by the four-bar linkage.

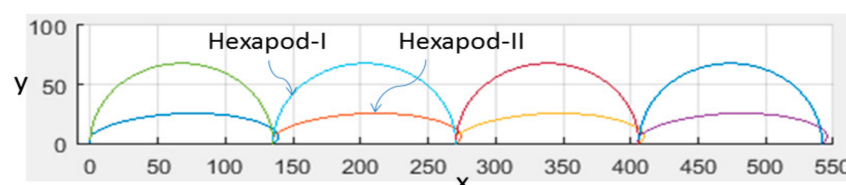


Figure 18. Loci of center of gravity: Hexapod-I versus Hexapod-II.

Note that the cost of a robot is generally proportional to the number of actuators. Therefore, the cost can be roughly estimated by counting the number of actuators. Taking a glimpse at Table 4, the numbers of actuators used by other hexapods are all much higher than the number of actuators used by our robots, i.e., Hexapod-I and Hexapod-II. This is due to the novelty of our approach, which uses

the mechanical mechanism rather than electronic circuits or computers to act as the CPG in achieving the locomotion.

7. Conclusions

According to neuroscience, a distributed control system is proposed for the locomotion of a legged robot, since the CPG, located in the spinal cord and in charge of the rhythmic motion, is an autonomous device, almost requiring neither the peripheral sensor feedback nor the regulation command from the brain-stem. A hexapod robot with biomimetic legs was built to realize such a distributed control system, where a mechanism is proposed to serve as the CPG and a computer to act as the brain-stem, wirelessly sending commands to the autonomous device. The proposed mechanism consists of two modules, i.e., the tripod gait generator and the Theo Jansen Linkage. The tripod gait generator is a device that uses a single motor to generate a tripod gait, while the TJL rhythmically executes the legged motion. The interesting point is that the complex mathematical function of the foot motion can be realized by the ensemble of links of the TJL. If the same function is executed by an electronic computer, it will require a great amount of the computational time and memory resources. Nevertheless, dimensioning the TJL appropriately is nontrivial, since the patterns of orbits generated by a TJL may vary according to its overall dimensions and can be cast into four groups: bell curves, ovals, sharp-pointed ovals, and lemniscates. In general, the ovals or bell orbits are legitimate, the sharp-pointed ovals are partly legitimate, while the lemniscates are illegitimate. Once the dimension of a TJL has been determined, it can generate an ellipse-like orbit with a transversal axis longer than the lateral axis, so as to achieve energy efficient walking.

Admittedly, the mechanical computer is inferior to the electronic computer in regards to flexibility. Therefore, in the future, efforts should be taken to introduce the adjustable mechanical structure to increase the adaptability of this line of approach. Although the proposed method is not suitable for the case of a legged robot, adapted to diversified terrain, it suits the case of a legged robot operating in a specific environment with relative unevenness, such as construction sites, where the grounds are somewhat muddy and rugged, or factories, where the floors are scattered with debris. Our aim is to build a hexapod robot for material handling, since using a legged robot as a mobile platform is still more effective than using a wheeled robot with regards to crossing obstacles and avoiding skidding.

Robots are, in fact, complex and expensive machines, consisting of many actuators, sensors, transmissions, and hardware. Designing a robot capable of especially excessive function can further increase its cost. The cost of building a robot is generally proportional to the number of actuators it uses. For instance, most hexapod robots, designed with collocated actuators, require 18 servos. Based on the design of non-collocated actuators, the proposed hexapod robot uses merely three motors. The value of this approach lies on the fact that it gives a way of building a hexapod robot with much low cost. The significance of this research is in employing a mechanical mechanism, rather than electronic circuits or computers, to act as the CPG in achieving locomotion.

Author Contributions: M.-C.H. designed the mechanism and F.L. built the mechatronic control system. J.Y. analyzed the kinematics of the Theo Jansen linkage and Y.L. developed the programs. M.-C.H. and F.L. contributed to realization and revision of the manuscript.

Funding: This research was funded by the Jiangxi University of Science and Technology, People's Republic of China (Grant No. jxxjbs18018).

Conflicts of Interest: The authors declare no conflicts of interest.

References

1. McGhee, R.B. Some finite state aspect of legged locomotion. *Math. Biosci.* **1968**, *2*, 67–84. [[CrossRef](#)]
2. McGhee, R.B.; Frank, A.A. On the stability properties of quadruped creeping gaits. *Math. Biosci.* **1968**, *3*, 331–351.
3. Orin, D. Interactive Control of a Six-Legged Vehicle with Optimization of Both Stability and Energy. Ph.D. Thesis, Ohio State University, Columbus, OH, USA, 1976.

4. Vukobratovic, M.; Juricic, D. Contribution to the synthesis of biped gait. *IEEE Trans. Biomed. Eng.* **1969**, *BME-16*, 1–6. [[CrossRef](#)]
5. Vukobratovic, M.; Borovac, B. Zero-moment point—Thirty five years of its life. *Int. J. Hum. Robot.* **2004**, *1*, 157–173. [[CrossRef](#)]
6. Bässler, U. On the Definition of Central Pattern Generator and its Sensory Control. *Biol. Cybern.* **1986**, *54*, 65–69. [[CrossRef](#)]
7. Matsuoka, K. Mechanism of Frequency and Pattern Control in the Neural Rhythm Generators. *Biol. Cybern.* **1987**, *56*, 345–353. [[CrossRef](#)] [[PubMed](#)]
8. Collins, J.J.; Richmond, S.A. Hard-Wired Central Pattern Generators for Quadrupedal Locomotion. *Biol. Cybern.* **1994**, *71*, 375–385. [[CrossRef](#)]
9. Ijspeert, A.J. Central Pattern Generators for Locomotion Control in Animals and Robots: A Review. *Neural Netw.* **2008**, *21*, 642–653. [[CrossRef](#)]
10. Yu, H.; Gao, H.; Ding, L.; Li, M.; Deng, Z.; Liu, G. Gait Generation with Smooth Transition Using CPG-Based Locomotion Control for Hexapod Walking Robot. *IEEE Trans. Ind. Electron.* **2016**, *63*, 5488–5500. [[CrossRef](#)]
11. Zhong, G.; Chen, L.; Jiao, Z.; Li, J.; Deng, H. Locomotion Control and Gait Planning of a Novel Hexapod Robot Using Biomimetic Neurons. *IEEE Trans. Control Syst. Technol.* **2018**, *26*, 624–636. [[CrossRef](#)]
12. Olsen, S.R.; Wilson, R.I. Cracking neural circuits in a tiny brain: New approaches for understanding the neural circuitry of *Drosophila*. *Trans. Trends Neurosci.* **2008**, *31*, 512–520. [[CrossRef](#)] [[PubMed](#)]
13. Ijspeert, A.J.; Crespi, A.; Cabelguen, J.M. Simulation and Robotics Studies of Salamander Locomotion. *Neuroinformatics* **2005**, *3*, 171–195. [[CrossRef](#)] [[PubMed](#)]
14. Aminzare, Z.; Srivastava, V.; Holmes, P. Gait transitions in a phase oscillator model of an insect central pattern generator. *SIAM J. Appl. Dyn. Syst.* **2018**, *17*, 626–671. [[CrossRef](#)]
15. Schilling, M.; Hoinville, T.; Schmitz, J. Walknet, a bio-inspired controller for hexapod walking. *Biol. Cybern.* **2013**, *107*, 397–419. [[CrossRef](#)]
16. Owaki, D.; Goda, M.; Miyazawa, S.; Ishiguro, A. A Minimal Model Describing Hexapodal Interlimb Coordination: The Tegotae-Based Approach. *Front. Neurobotics* **2017**, *11*, 1–13. [[CrossRef](#)] [[PubMed](#)]
17. Romano, D.; Donati, E.; Benelli, G.; Stefanini, C. A review on animal–robot interaction: From bio-hybrid organisms to mixed societies. *Biol. Cybern.* **2019**, *113*, 201–225. [[CrossRef](#)] [[PubMed](#)]
18. Romano, D.; Benelli, G.; Stefanini, C. Encoding Lateralization of Jump Kinematics and Eye Use in a Locust via Bio-Robotic Artifacts. *J. Exp. Biol.* **2019**, *222*, jeb187427. [[CrossRef](#)]
19. Strandbeest Evolution 2018. Available online: <http://www.strandbeest.com/> (accessed on 18 October 2018).
20. Komoda, K.; Wagatsums, H. A Proposal of the extended mechanism for Theo Jansen linkage to modify the walking elliptic orbit and a study of cyclic bas function. In Proceedings of the 7th Annual Dynamic Walking Conference, Pensacola, FL, USA, 21 February 2012; pp. 2–4.
21. Nansai, S.; Rajesh, M.; Iwase, M. Dynamic Analysis and Modeling of Jansen Mechanism. *Procedia Eng.* **2013**, *64*, 1562–1571. [[CrossRef](#)]
22. Komoda, K.; Wagatsuma, H. Singular Configurations Analyses of the Modifiable Theo Jansen-like Mechanism by Focusing on the Jacobian determinant—A Finding Limitations to Exceed Normal Joint Range of Motion. In Proceedings of the 2014 IEEE/ASME International Conference on Advanced Intelligent Mechatronics, Besançon, France, 8–11 July 2014; pp. 76–81.
23. Mohsenizadeh, M.; Zhou, J. Kinematic Analysis and Simulation of Theo Jansen Mechanism. In Proceedings of the Fifteenth Annual Early Career Technical Conference, Tuscaloosa, AL, USA, 7–8 November 2015; pp. 97–104.
24. Nansai, S.; Mohan, R.E.; Tan, N.; Rojas, N.; Iwase, M. Dynamic Modeling and Nonlinear Position Control of a Quadruped Robot with Theo Jansen Linkage Mechanisms and a Single Actuator. *J. Robot.* **2015**, *2015*, 1–15. [[CrossRef](#)]
25. Nansai, S.; Rajesh Elara, M.; Iwase, M. Speed Control of Jansen Linkage Mechanism for Exquisite Tasks. *J. Adv. Simul. Sci. Eng.* **2016**, *3*, 47–57. [[CrossRef](#)]
26. Denavit, J.; Hartenberg, R.S. A Kinematic Notation for Lower-Pair Mechanisms Based on Matrices. *ASME J. Appl. Mech.* **1955**, *77*, 215–221.
27. Arduino. Available online: <https://www.arduino.cc/> (accessed on 1 June 2019).
28. Peternella, M.; Salinari, S. Simulation by digital computer of walking machine control system. In Proceedings of the 5th IFAC Symposium on Automatic Control in Space of the Conference, Genova, Italy, 4–8 June 1973.

29. Delcomyn, F.; Nelson, M.E. Architectures for a biomimetic hexapod robot. *Robot. Auton. Syst.* **2000**, *30*, 5–15. [[CrossRef](#)]
30. Fielding, M.R.; Dunlop, R.; Damaren, C.J. Hamlet: Force/Position controlled hexapod walker—Design and systems. In Proceedings of the IEEE Conference on Control Applications, Mexico City, Mexico, 5–9 September 2001; pp. 984–989.
31. Saranli, U.; Buehler, M.; Koditschek, D.E. RHex—A simple and highly mobile hexapod robot. *Int. J. Robot. Res.* **2001**, *20*, 616–631. [[CrossRef](#)]
32. Cham, J.G.; Bailey, S.A.; Clark, J.E.; Full, R.J.; CutKosky, M.R. Fast and robust: Hexapodal robots via shape deposition manufacturing. *Int. J. Robot. Res.* **2002**, *21*, 869–882. [[CrossRef](#)]
33. Brooks, R.A. A robot that walks; emergent behaviors from a carefully evolved network. *Neural Comput.* **1989**, *1*, 253–262. [[CrossRef](#)]
34. Lewinger, W.A.; Branicky, M.S.; Quinn, R.D. Insect-inspired, actively compliant hexapod capable of object manipulation. In Proceedings of the 8th International Conference on Climbing and Walking Robots, London, UK, 13–15 September 2005; pp. 65–72.
35. Arena, P.; Fortuna, L.; Frasca, M.; Patane, L.; Pavone, M. Implementation and experimental validation of an autonomous hexapod robot. In Proceedings of the IEEE International Symposium on Circuits and Systems, Kos, Greece, 21–24 May 2006.
36. Asbeck, A.T.; Kim, S.; McClung, A.; Parness, A.; Cutkosky, M.R. Climbing walls with microspines. In Proceedings of the IEEE International Conference Robotics and Automation, Orlando, FL, USA, 15–19 May 2006.
37. Hwang, M.C.; Huang, C.J.; Liu, F.F. A Hexapod Robot with Non-Collocated Actuators. *Appl. Syst. Innov.* **2018**, *1*, 20. [[CrossRef](#)]



© 2019 by the authors. Licensee MDPI, Basel, Switzerland. This article is an open access article distributed under the terms and conditions of the Creative Commons Attribution (CC BY) license (<http://creativecommons.org/licenses/by/4.0/>).